DOI: 10.1002/((please add manuscript number))
Article type: Communication

High Performance Deep-Red/Near-Infrared OLEDs with Tetradentate [Pt(O^N^C^N)] Emitters

*Gang Cheng, Qingyun Wan, Wai-Hung Ang, Chun-Lam Kwong, Wai-Pong To, Pui-Keong Chow, Chi-Chung Kwok, and Chi-Ming Che**

Dr. G. Cheng, Q. Wan, W.-H. Ang, C.-L. Kwong, Dr. W.-P. To, Dr. P.-K. Chow, Dr. C.-C. Kwok, Prof. C.-M. Che
State Key Laboratory of Synthetic Chemistry, Institute of Molecular Functional Materials, and Department of Chemistry, The University of Hong Kong, Pokfulam Road, Hong Kong SAR, China
E-mail: cmche@hku.hk

Dr. G. Cheng, Prof. C.-M. Che
HKU Shenzhen Institute of Research and Innovation, Shenzhen 518053, China

Keywords: platinum(II) complexes, deep-red emission, near-infrared emission, aggregation forms, organic light-emitting devices

Abstract: The emission properties of two series of tetradentate Pt(II) emitters in aggregation forms are studied by Density Functional Theory (DFT), Time Dependent DFT (TD-DFT) calculations and photoluminescence (PL) measurements. PL quantum yields (PLQYs) of the complexes bearing type-I O^N^C^N ligands (**Pt-X-1** and **Pt-X-2**) increase with the dopant concentration in thin film until 100% [pristine Pt(II) complexes]. For complexes bearing type-II O^N^C^N ligands (**Pt-X-3** to **Pt-X-5**), their PLQYs in thin film increase as the dopant concentration increases up to a certain threshold and then quickly decrease with further increase in dopant concentration. Organic light-emitting devices (OLEDs) with neat and doped Pt(II) emitters are fabricated and characterized. High efficiency near-infrared OLEDs with λ_{max} exceeding 700 nm and EQEs of up to 15.84% are realized by using a neat **Pt-X-1** thin film as the emitting layer (EML). For this device, a high EQE of 11.19% is retained at high current density of 100 mA cm^{-2}; by doping **Pt-X-5 (**26 wt%) into a co-host structure EML, a red emission with λ_{max} of 661 nm, CIE coordinates of (0.63, 0.37) and EQE of 21.75% at 1000 cd m^{-2} are achieved.

Deep-red and near-infrared (NIR) organic light-emitting devices (OLEDs) have important, useful applications in biomedicines, security and communications.[1] To date, several types of deep-red and/or NIR OLEDs based on phosphorescent transition-metal complexes,[2] fluorescent organic dyes,[3, 4] luminescent lanthanide complexes[5] and conjugated polymers[6] have been reported. With pincer [Pt^{II}(N^C^N)] complexes [N^C^N=C-deprotonated 1,3-di(2-pyridyl)benzene] as the emitting layer (EML),[7] Cocchi and co-workers demonstrated NIR OLEDs having external quantum efficiencies (EQEs) of up to 14.5% and emission maxima (λ_{max}) of up to 700 nm.[2c] Utilizing the π-extended Pt(II) porphyrin Pt-Ar_4TBP [Ar_4TBP = 5,10,15,20-(3,5-di-*tert*-butylphenyl)tetrabenzoporphyrinato dianion], Reynolds and co-workers reported NIR OLEDs having EQEs of up to 9.2% and λ_{max} at 773 nm.[2e] Nonetheless, the EQE of these NIR devices quickly dropped with increasing current as a result of the long emission lifetimes (τ_{em}) of these Pt(II) complexes. For instance, the τ_{em} of Pt-Ar_4TBP is as long as 32.0 μs in toluene solution.[2e] To suppress the pronounced efficiency roll-off of phosphorescent deep-red/NIR OLEDs, fluorescent organic dyes, including those capable of harnessing triplet excitons *via* triplet fusion[3c] or "hot exciton"[3b] processes, have been developed. Nonetheless, the EQEs of the deep-red/NIR OLEDs based on these fluorescent dyes are generally less than 3%. Recently, with the rapid development of thermally activated delayed fluorescent (TADF) materials, highly efficient NIR OLEDs have been documented in literatures.[4] By using $Zn(BTZ)_2$ as a host material, OLEDs based on a TADF emitter, 3,4-bis(4-(diphenylamino)phenyl)acenaphtho[1,2-b]pyrazine-8,9-dicarbonitrile (APDC-DTPA), displayed NIR emission with maximum EQE of 7.8% and λ_{max} at 710 nm.[4f] Meanwhile, Adachi and co-workers demonstrated NIR TADF-OLEDs having maximum EQE approaching 10% and λ_{max} at 721 nm by using a boron difluoride curcuminoid derivative as a emitting dye and 4,4′-bis(N-carbazolyl)-1,10-biphenyl (CBP) as a host.[4e] The efficiency roll-off at high current density for these NIR devices have been found to be significant presumably due to the relatively long τ_{em} of the TADF materials used. When compared to the best

reported blue, green and red OLEDs, the EQEs of which are typically over 30%,[8] the performance of deep-red/NIR OLEDs are far inferior. The design of deep-red/NIR emitters having high emission quantum yields (Φ_{em}) faces a formidable challenge as, according to the energy gap law, the non-radiative rate constant (k_{nr}) would increase exponentially with decrease in the energy gap (ΔE) between the emissive excited state and ground state.[9]

It has been well documented that the emission of Pt(II) complexes in aggregation forms is pronouncedly red shifted from that in mononuclear forms.[2a, 2c] Notably, the τ_{em} values of aggregated Pt(II) complexes are usually short (typically 0.1-1 μs)[10] with corresponding radiative decay rate constants (k_r) being large, thereby able to minimize the effect due to the increase in k_{nr} as a result of the energy gap law. With the reduction in triplet-triplet annihilation and/or saturation of excited states, the short τ_{em} of Pt(II) complexes in aggregation forms is useful in resolving the efficiency roll-off issue that is notoriously difficult to be resolved in the development of high performance phosphorescent and TADF deep-red/NIR OLEDs.[1, 2, 4, 11] Recently, a few Pt(II) complexes have been reported to exhibit high photoluminescence quantum yield (PLQY), short τ_{em} and/or a horizontally oriented emitting dipole in the neat state. Utilizing the emission of these Pt(II) complexes in neat thin films, high performance non-doped OLEDs were successfully fabricated.[8c, 10, 13] An EQE of up to 38.8% was achieved for the red-emitting electroluminescent (EL) device fabricated with a crytalline, thin film of bis(3-(trifluoromethyl)-5-(2-pyridyl)-pyrazolate)platinum(II) as the emitter.[8c] Very recently, highly efficient NIR OLEDs having EQEs of up to 24% and λ_{max} at 740 nm were obtained using neat 2-pyrazinyl pyrazolate Pt(II) complexes as emitter in a normal planar organic device structure.[12a] Nonetheless, most Pt(II) complexes in neat thin film usually display fairly low PLQYs due to intermolecular photon interactions and an overall decrease in the oscillator strength of electronic transitions.[14] Alternatively, Kido and co-workers demonstrated deep-red OLEDs with high EQEs of up to 18% and λ_{max} of 670 nm

by using energy transfer from an exciplex host to a deep-red phosphorescent emitter, (DPQ)2Ir(dpm).[12b]

In the present study, two series of [Pt(O^N^C^N)] (O^N^C^N = C-deprotonated 5,5-dialkyl-2-(3-(pyridin-2-yl)-phenyl)-5H-indeno[1,2-b]pyridin-9-olates and their analogues) complexes, (**Pt-X-1** and **Pt-X-2**)[15] and (**Pt-X-3** to **Pt-X-5**)[16] (**Scheme 1**), were used as emitting materials in both doped and non-doped OLEDs. OLEDs with high EQE values and low efficiency roll-off have been realized by harnessing the intermolecular interactions of all these Pt(II) complexes in co-host device structure. For the devices with neat [Pt(O^N^C^N)] complexes as emitting layer (EML), high efficiency emission was only realized with those bearing type-I O^N^C^N ligands (**Pt-X-1** and **Pt-X-2**). The different behaviors between these two series of Pt(II) complexes in aggregation forms were investigated by photo-physical studies and theoretical calculations. NIR OLEDs with λ_{max} exceeding 700 nm and EQEs of up to 15.84% were fabricated by using a neat **Pt-X-1** thin film as the EML. For this device, a high EQE of 11.19% was retained at a high current density of 100 mA cm^{-2}. By doping **Pt-X-5** (26 wt%) into a co-host structure EML, a red emission with a λ_{max} of 661 nm, CIE coordinates of (0.63, 0.37) and EQE of 21.75% at 1000 cd m^{-2} were achieved.

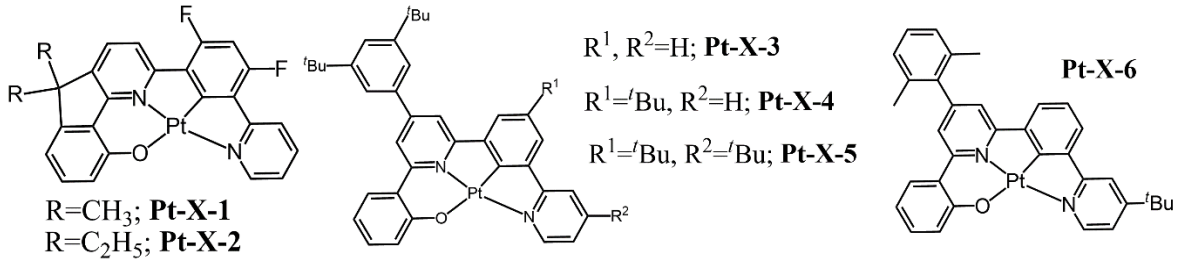

Scheme 1. Chemical structures for **Pt-X-1** to **Pt-X-6**

The Pt(II) complexes bearing type-I O^N^C^N ligands, **Pt-X-1** and **Pt-X-2**, have been reported as single emitter material for white OLEDs.[15] The alkyl chains of type-I O^N^C^N ligands are orthogonal to the [Pt(O^N^C^N)] motif, thereby preventing the intermolecular interactions and formation of aggregates. Density functional theory (DFT) calculations were performed to calculate the structures of dimers for **Pt-X-1** and **Pt-X-2**. As depicted in **Figure**

1, two triplet excited states, T_{1a} and T_{1b}, with different intermolecular Pt-Pt distances were found and optimized for both [**Pt-X-1**]$_2$ and [**Pt-X-2**]$_2$. A significant Pt-Pt bonding interaction has been observed between two Pt atoms in the T_{1a} state, as revealed by the large contraction of the Pt-Pt distance upon photo-excitation. In the T_{1b} state, the Pt-Pt distance is substantially longer. The energy difference between T_{1a} and T_{1b} was calculated to be 9.5 kcal mol^{-1} for **Pt-X-1** and 5.8 kcal mol^{-1} for **Pt-X-2**.

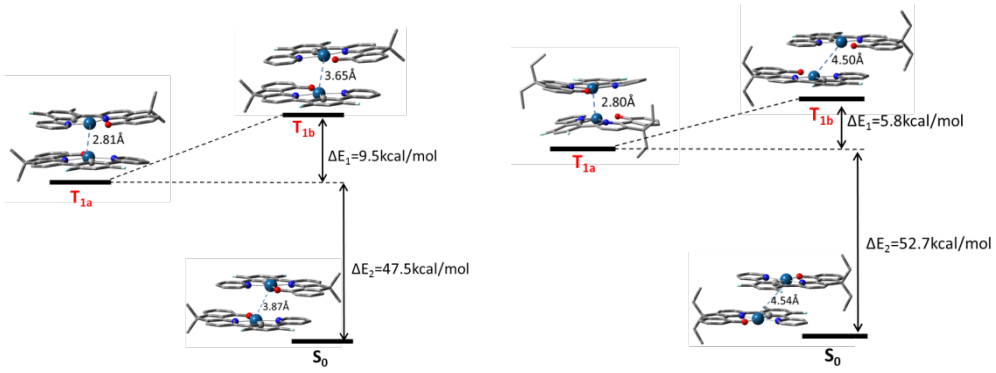

Figure 1. Optimized structures of dimers for **Pt-X-1** (left) and **Pt-X-2** (right) at singlet ground state S_0 and triplet excited state T_{1a}, T_{1b}.

TDDFT calculations were performed on both the T_{1a} and T_{1b} states of [**Pt-X-1**]$_2$ and [**Pt-X-2**]$_2$. The calculated emission energies for T_{1a} and T_{1b} states of [**Pt-X-1**]$_2$ are 703 and 558 nm, respectively. For [**Pt-X-2**]$_2$, the calculated emission energies are 671 nm for T_{1a} and 476 nm for T_{1b}. The low energy emission of [**Pt-X-1**]$_2$ and [**Pt-X-2**]$_2$ is assigned to T_{1a} states having mixed excimer $^3\pi$-π^* and ^{3}MMLCT characters as a result of intermolecular bonding interactions. The frontier molecular orbitals (FMOs) of [**Pt-X-1**]$_2$ and [**Pt-X-2**]$_2$ as a function of intermolecular distance are given in **Figure S1** of the Supporting Information. For the T_{1b} state of [**Pt-X-2**]$_2$, with an intermolecular separation of 4.5 Å, the emission is similar to that of **Pt-X-2** in the monomeric form. This is consistent with the observations that the HOMO in the dimeric structure is localized on only one molecule. At a shorter intermolecular separation, the emission is derived from the aggregation form(s), the FMOs of which are delocalized on both monomers. Both inter-ligand π-π and Pt-Pt interactions contribute to the aggregation,

which is supported by the compositions of the FMOs. With further decreasing intermolecular distances, the Pt(II)-Pt(II) orbital interaction and Pt(II)/ligand-ligand dispersion interactions increase, thereby narrowing the HOMO and LUMO energy gap for both **Pt-X-1** and **Pt-X-2**.

The photo-physical properties of **Pt-X-1** and **Pt-X-2** in dilute solutions[15] as well as high performance OLEDs based on complexes **Pt-X-1** to **Pt-X-5** in monomeric form have been reported.[16] In this work, the photo-physical properties of **Pt-X-1** to **Pt-X-5** dispersed in PMMA thin films at various dopant concentrations were measured. In these experiments, the concentration was defined as the ratio of dopant weight to total weight of host and dopant, *i.e.*, $W_{dopant}/(W_{dopant}+W_{host})$. Thus, the 100 wt% case was neat Pt(II) complex without PMMA. **Figure 2**a depicts the dependence of the intensity ratio of aggregation emission (I_{agg}) to the total emission ($I_{mono}+I_{agg}$), where I_{mono} represents emission from **Pt-X-1** to **Pt-X-5** in monomeric form. The $I_{agg}/(I_{mono}+I_{agg})$ ratio was found to quickly increase with dopant concentration approaching unity at a threshold concentration as depicted in **Figure S3**, Supporting Information. The threshold concentrations (between 20 and 40 wt%) for **Pt-X-1** to **Pt-X-5** were proposed to have correlation with the intermolecular interactions of the Pt(II) complex. Based on our calculations (Figure S1, Supporting Information), for the Pt(II) complexes in aggregation forms having varying intermolecular Pt-Pt distances, their HOMO-LUMO gaps would be narrowed down with the decrease in the Pt-Pt distance, as depicted in Figure S3, Supporting Information, indicating the red-shift of the emission energy upon excitation. The dependence of PLQY upon dopant concentration for **Pt-X-1** to **Pt-X-5** in thin films is depicted in Figure 2b. For **Pt-X-1** and **Pt-X-2** thin films, the PLQYs increased with dopant concentration until 40 wt% and then remained almost unchanged up to 100 wt%. The high PLQYs for **Pt-X-1** and **Pt-X-2** at high dopant concentrations may be the result of a short emission lifetime for the ^{3}MMLCT emission when the Pt(II) complex is in aggregation form(s), as presented in **Table S1**, Supporting Information.[10] For thin films of **Pt-X-3** to **Pt-X-5**, the PLQYs increased to a maximum value at a medium dopant concentration (Φ_{em} was

0.525 for 5 wt% **Pt-X-3**, 0.483 for 10 wt% **Pt-X-4** and 0.550 for 5 wt% **Pt-X-5**, respectively) and then quickly dropped up to 100 wt%. The PLQYs became quite low for **Pt-X-3** to **Pt-X-5** in neat films. It is notable that with increasing $I_{agg}/(I_{mono}+I_{agg})$ emission ratios, the PLQYs of Pt(II) complexes bearing type-I O^N^C^N ligand (**Pt-X-1** and **Pt-X-2**) are higher than those bearing type-II O^N^C^N ligand (**Pt-X-3** to **Pt-X-5**). For instance, PLQY is, respectively, 0.676 and 0.739 for neat **Pt-X-1** and **Pt-X-2** films, while this value is much lower for those of **Pt-X-3** (0.199), **Pt-X-4** (0.075) and **Pt-X-5** (0.121).

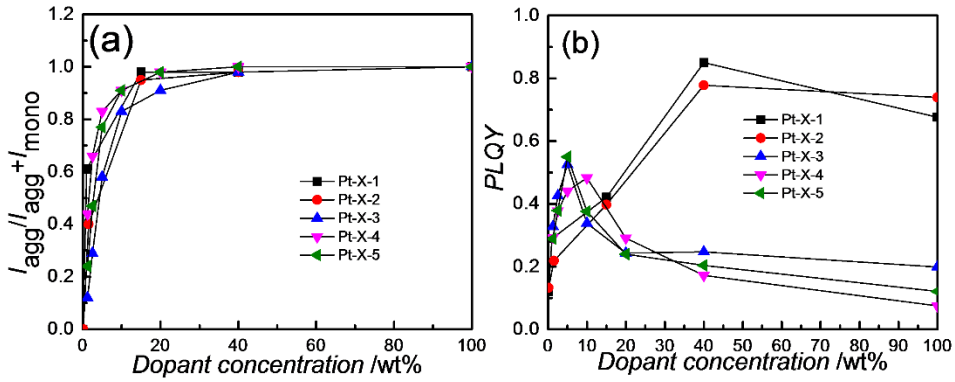

Figure 2. The dependence of (a) $I_{agg}/(I_{mono}+I_{agg})$ and (b) PLQY upon dopant concentration for **Pt-X-1** to **Pt-X-5**.

To understand the low PLQY value of neat Pt(II) complexes bearing type-II O^N^C^N ligand (**Pt-X-3** to **Pt-X-5)**, DFT calculations were performed on the singlet ground and triplet excited states of dimer [**Pt-X-3**]$_2$. Similar to those of [**Pt-X-1**]$_2$ and [**Pt-X-2**]$_2$, two triplet excited states, T_{1a} with dominated Pt-Pt interaction and T_{1b} with dominated π-π interaction have been found in [**Pt-X-3**]$_2$. According to our calculations, for [**Pt-X-3**]$_2$, the angle of the labeled atoms Pt, N and C (**Figure S2**a) decreases from 173° in S_0 to 162° in T_{1a} while the one in T_{1b} shows slight variation only. Since the amplitude of structural distortion could be correlated to the value of k_{nr}, a larger k_{nr} is anticipated for the facile decay of excited state T_{1a} to ground state S_0, thereby lowering the PLQY of closely packed neat thin film of **Pt-X-3**. Such structural distortion could be mainly due to the two tertiary butyl groups on type-II O^N^C^N ligands that also exist in **Pt-X-4** and **Pt-X-5** and could be responsible for their low

PLQY in neat film states. Thus, the PLQY of this type of Pt(II) complexes could be improved by removing these two tertiary butyl groups. **Pt-X-6** was therefore synthesized by replacing these two tertiary butyl groups at the *meta*-positions with two methyl groups at the *ortho*-positions (Scheme 1); the presence of methyl groups at the *ortho*-positions could minimize the rotation of the phenyl ring. As expected, the PLQY of **Pt-X-6** neat thin film is improved to 0.42 (**Table S2**, Supporting Information).

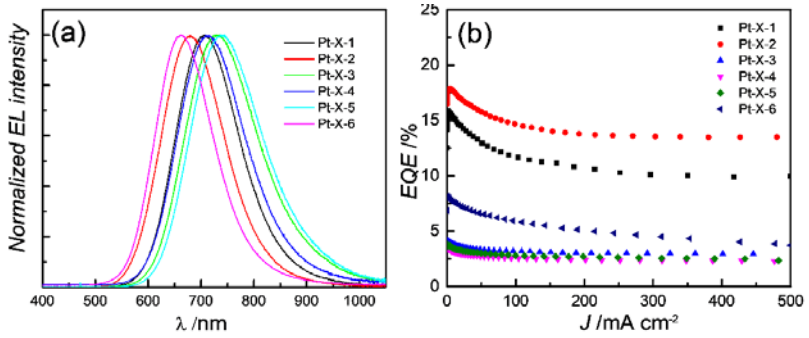

Figure 3. (a) Normalized EL spectra at 100 mA cm^{-2} and (b) EQE-current density (*J*) characteristics of NIR OLEDs with neat **Pt-X-1** to **Pt-X-6** as the EML.

The electroluminescence (EL) properties of neat **Pt-X-1** to **Pt-X-6** were investigated in OLEDs with the architecture of ITO/MoO_3 (2 nm)/TAPC (40 nm)/TCTA (10 nm)/EML (30 nm)/B3PYMPM (50 nm)/LiF (1.2 nm)/Al (100 nm). 1,1-Bis-(4-bis(4-methylphenyl)-amino-phenyl)-cyclohexane (TAPC) was used as a hole transporting layer (HTL), 4,4′,4″-tris(*N*-carbazolyl)-triphenylamine (TCTA) as an electron/excition blocking layer (EBL) and bis-4,6-(3,5-di-3-pyridylphenyl)-2-methylpyrimidine (B3PYMPM) as an electron transporting layer (ETL). Thin film of neat Pt(II) complex **(Pt-X-1** to **Pt-X-6)** was used as EML. Normalized EL spectra of **Pt-X-1** to **Pt-X-6** devices are depicted in **Figure 3**a. The EL λ_{max} of **Pt-X-1**, **Pt-X-2**, **Pt-X-3**, **Pt-X-4, Pt-X-5** and **Pt-X-6** devices are at 707, 679, 730, 716, 739 and 667 nm, respectively. The devices with **Pt-X-1**, **Pt-X-3**, **Pt-X-4** and **Pt-X-5** can be classified as NIR OLEDs whose emission λ_{max} exceed 700 nm,[2i-2l, 4e, 12] while those with **Pt-X-2** and **Pt-X-6** deep-red OLEDs. The EQE-current density characteristics of the **Pt-X-1** to **Pt-X-6** devices are depicted in **Figure 3**b. EQE of 17.89% for the deep-red **Pt-X-2** device is the highest among

those of non-doped OLEDs studied in this work, and this can be accounted for by the highest PLQY (73.9%) of neat **Pt-X-2** (**Table S2**, Supporting Information). Among these NIR OLEDs, the highest EQE of 15.84% was achieved with the neat **Pt-X-1** device. More importantly, the efficiency roll-off of this device is low and the EQE of 11.19% retains at high current density of 100 mA cm^{-2}.

Compared to those of **Pt-X-1** and **Pt-X-2**, the efficiencies of non-doped OLEDs based on **Pt-X-3** to **Pt-X-5** are lower attributable to the lower PLQYs of these complexes in neat thin films, as presented in Figure 2b. Nonetheless, the PLQYs of **Pt-X-3** to **Pt-X-5** doped into PMMA film are much higher and hence high-efficiency OLEDs with **Pt-X-3** to **Pt-X-5** as the emitting dopant may be expected. We therefore fabricated and characterized doped OLEDs with the architecture of ITO/MoO_3(2 nm)/TAPC(40 nm)/TCTA(10 nm)/TCTA:B3PYMPM:emitter (30 nm)/B3PYMPM (50 nm)/LiF (1.2 nm)/Al (100 nm). TAPC, TCTA and B3PYMPM were used as HTL, EBL and ETL, respectively. The exciplex-forming co-host consisting of TCTA:B3PYMPM in a 1:1 molar ratio was used in the EML.[8a, 18] Complexes **Pt-X-1** to **Pt-X-5** were used as the emitting dopant with concentration varying from less than 10 wt% to ~50 wt% in order to investigate the EL properties of these Pt(II) complexes in both monomer and aggregation forms. Here, the dopant concentration was calculated by $W_{dopant}/(W_{dopant}+W_{host})$. The dependence of $I_{agg}/(I_{agg}+I_{mono})$ upon dopant concentration for **Pt-X-1** to **Pt-X-5** devices is presented in **Figure 4**a and the corresponding spectra are depicted in **Figure S4**, Supporting Information. Similar to the PL of **Pt-X-1** to **Pt-X-5** dispersed in PMMA (Figure 2a), the $I_{agg}/(I_{agg}+I_{mono})$ values for the EL spectra of these Pt(II) complexes increased with increasing dopant concentration until the monomer emission vanished (I_{mono} ~0) at a threshold value (33 wt% for **Pt-X-1**, 50 wt% for **Pt-X-2**, 40 wt% for **Pt-X-3**, 40 wt% for **Pt-X-4** and 43 wt% for **Pt-X-5**). The EL of the doped OLEDs blue-shifted compared to those of the non-doped OLEDs for all the Pt(II) complexes, which may be accounted for by the longer intermolecular Pt-Pt distances when the Pt(II) complex was

dispersed in the host. This phenomenon is in agreement with the results of the calculations presented in Figure S1, Supporting Information. The dependence of EQEs of the doped OLEDs with **Pt-X-1** to **Pt-X-5** on dopant concentration is shown in Figure 4b. Key performance data of **Pt-X-1** to **Pt-X-5** devices are summarized in **Table 1**. Compared to the relatively low EQEs of OLEDs based on Pt(II) complex in neat form, especially those of **Pt-X-3**, **Pt-X-4** and **Pt-X-5**, the performances of OLEDs with Pt(II) dopant in co-host EMLs have been greatly improved. Among the red devices, the one with 26 wt% **Pt-X-5** showed the best performance; an EQE of 21.75% and a λ_{max} of 661 nm at 1000 cd m^{-2} were achieved (**Figure 5** and Table 1). The weak emission at around 530 nm in the EL of this device was originated from the monomer emission of **Pt-X-5**. Such emission broadened the EL spectrum, leading to a CIE coordinates of (0.63, 0.37). The monomer emission could be eliminated by further increasing the dopant concentration of **Pt-X-5** as depicted in Figure S4, Supporting Information, and the color purity was therefore improved to (0.65, 0.35) in the device with 43 wt% **Pt-X-5** (see Table 1).

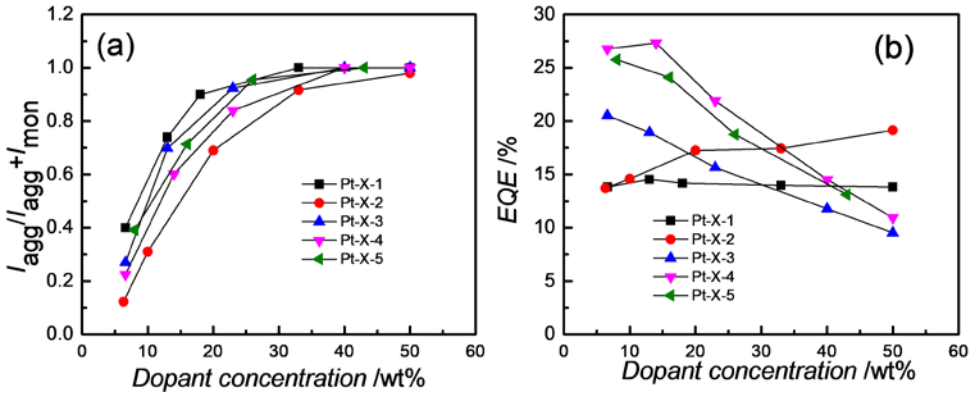

Figure 4. (a) The intensity ratio of aggregation emission to total emission for the OLEDs with **Pt-X-1** to **Pt-X-5** at different dopant concentrations. (b) The dependence of the EQE of **Pt-X-1** to **Pt-X-5** OLEDs on dopant concentration at 1000 cd m^{-2}.

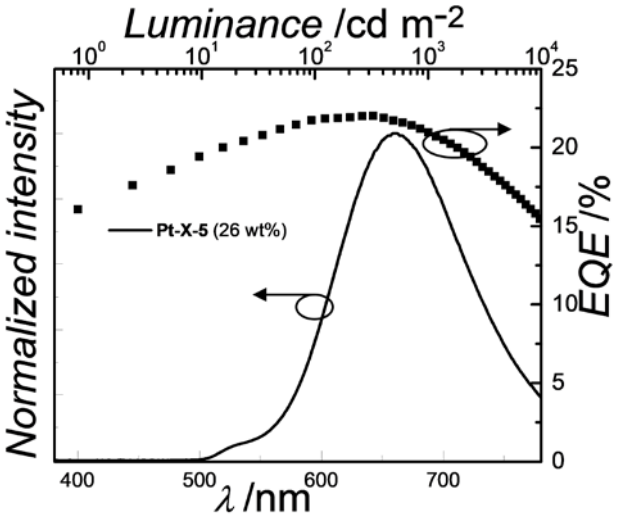

Figure 5. Normalized EL spectra and EQE-luminance characteristics of OLEDs with 26 wt% **Pt-X-5**.

Table 1. Selected performances of OLEDs with **Pt-X-1** to **Pt-X-5**

Complex (wt%)	L [cd m^{-2}] [a]	V_{on} [V][b]	CE [cd A^{-1}][c]		PE [lm W^{-1}][d]		EQE [%][e]		PLQY [%][f]	CIE [(x, y)]; λ_{max} [nm][g]
			Max	at 1000 cd m^{-2}	Max	at 1000 cd m^{-2}	Max	at 1000 cd m^{-2}		
Pt-X-1 (6.6)	13000	2.5	28.05	25.75	28.31	16.39	15.87	13.82	62.9	(0.38, 0.48); 512, 640
Pt-X-1 (13)	21450	2.7	18.26	18.13	16.03	11.16	15.17	14.54	61.8	(0.51, 0.43); 512, 650
Pt-X-1 (18)	28570	2.7	13.50	13.44	13.90	8.52	14.23	14.19	61.3	(0.57, 0.40); 512, 660
Pt-X-1 (33)	39170	2.8	9.90	9.78	7.03	4.44	14.95	13.97	59.6	(0.62, 0.38); 670
Pt-X-1 (50)	45340	2.9	8.64	8.63	6.46	3.40	14.60	13.82	58.4	(0.64, 0.36); 670
Pt-X-2 (6.6)	11000	2.5	43.39	35.43	52.80	23.97	16.88	13.71	65.5	(0.26, 0.53); 513
Pt-X-2 (10)	13100	2.5	34.49	31.18	37.53	20.65	16.59	14.59	68.4	(0.34, 0.50); 513, 628
Pt-X-2 (20)	17800	2.5	28.45	27.39	24.95	16.91	17.68	17.25	73.5	(0.49, 0.44); 513, 630
Pt-X-2 (33)	30000	2.6	23.06	22.83	18.96	10.67	18.15	17.43	79.5	(0.58, 0.40); 513, 642
Pt-X-2 (50)	55500	2.7	19.96	19.85	16.98	9.92	19.53	19.15	85.2	(0.61, 0.38); 644
Pt-X-3 (6.6)	43050	2.5	47.95	47.22	42.71	33.54	20.61	20.53	80.4	(0.37, 0.59); 522, 653
Pt-X-3 (13)	49400	2.5	22.56	21.78	16.01	13.09	19.02	18.94	74.1	(0.48, 0.50); 530, 665
Pt-X-3 (23)	43550	2.7	10.77	10.68	8.38	5.69	16.56	15.64	65.8	(0.58, 0.41); 530, 671
Pt-X-3 (40)	28250	2.7	5.57	5.63	4.54	2.49	12.23	11.77	54.0	(0.63, 0.35); 681
Pt-X-3 (50)	23700	2.7	4.36	4.42	3.37	1.92	10.11	9.53	48.2	(0.65, 0.35); 683
Pt-X-4 (6.6)	68050	2.3	79.09	77.44	68.70	58.50	26.94	26.77	96.3	(0.39, 0.59); 527
Pt-X-4 (14)	89040	2.3	53.95	50.00	36.56	32.89	27.43	27.32	92.2	(0.48, 0.50); 531, 649
Pt-X-4 (23)	71140	2.3	28.47	27.82	21.25	15.93	21.93	21.90	81.5	(0.58, 0.41); 651
Pt-X-4 (40)	44000	2.5	9.42	9.32	9.93	4.34	15.73	14.52	63.2	(0.65, 0.35); 661
Pt-X-4 (50)	29200	2.6	7.12	7.05	6.48	2.78	11.76	10.94	52.4	(0.66, 0.34); 664
Pt-X-5 (8)	70500	2.5	54.64	51.59	44.84	37.11	25.82	25.76	86.8	(0.44, 0.54); 529, 649
Pt-X-5 (16)	72000	2.5	32.12	29.79	23.78	19.81	24.16	24.11	82.3	(0.54, 0.45); 531, 654
Pt-X-5 (26)	48750	2.5	16.18	16.49	11.30	80.9	22.02	21.75	79.2	(0.63, 0.37); 661
Pt-X-5 (43)	41800	2.5	9.08	9.07	7.09	4.04	13.76	13.10	60.5	(0.65, 0.35); 667

[a] Maximum luminance; [b] turn-on voltage, the driving voltage at 1 cd m^{-2}; [c] current efficiency; [d] power efficiency; [e] external quantum efficiency calculated within visible spectrum region; [f] PLQY of thin film sample in TCTA: B3PYMPM co-host; [g] CIE coordinates and EL maxima at 1000 cd m^{-2}.

The EQE value is mainly determined by PLQY and the out-coupling efficiency for properly designed phosphorescent OLEDs.[19] The out-coupling efficiency is strongly influenced by the horizontal transition dipole moment of the EML and could be over 40% when the horizontal dipole ratio (Θ) of EML is approaching unity.[8a] High Θ values of 93% and 87% have been respectively observed in neat $Pt(fppz)_2$ and $Pt(fprpz)_2$ thin films attributed to their highly preferred horizontal oriented dipoles.[12, 8c] In our case, for the OLEDs based on neat **Pt-X-1**, **Pt-X-2** and **Pt-X-6**, the out-coupling efficiencies were respectively 23.43, 24.21, and 19.6% estimated by the EQE and PLQY values listed in **Table S2**, Supporting Information.[19] These findings indicate that the emission dipoles of **Pt-X-1** and **Pt-X-2** may be horizontally aligned (Θ >0.67) while that of **Pt-X-6** could be isotropically oriented (Θ = 0.67). To estimate the out-coupling efficiency of the devices doped with **Pt-X-1** to **Pt-X-5**, the corresponding thin flims of **Pt-X-1** to **Pt-X-5** in the TCTA: B3PYMPM co-host were prepared and subjected to PLQY measurements. The results are listed in Table 1. The estimated out-coupling efficiencies of doped devices are typically between 20% and 30%, higher than those of the non-doped devices, probably attributed to the horizontally aligned co-host TCTA: B3PYMPM (Θ > 0.67) used.[8a, 18]

Preliminary study on the relative operational stability of OLEDs with neat and doped **Pt-X-3** was undertaken under our laboratory conditions**.** The device structures were the same as the aforementioned corresponding ones. The lifetimes at 90% initial luminance (LT_{90}, L_0 = 100 cd m^{-2}) of the co-doped OLEDs with 10 wt% **Pt-X-3** and 30 wt% **Pt-X-3** were 59 and 374 h, respectively, as depicted in **Figure S10**, Supporting Information. The increased stability of the device with **Pt-X-3** doped in higher concentration suggests that the aggregation form may improve the device stability. For the non-doped device with neat **Pt-X-3**, the lifetime was much shorter with LT_{90} of 1.17 h (L_0 = 100 cd m^{-2}). This could be due to the low EQE (less than 3%) of the non-doped device with **Pt-X-3** and/or the imbalance charge-transfer property of the neat **Pt-X-3** EML. [20]

In conclusion, the [Pt (O^N^C^N)] complexes **Pt-X-1** to **Pt-X-5** in aggregation forms were studied by DFT/TDDFT calculations and photo-physical measurements revealing the presence of significant intermolecular interactions in the solid state. The PLQYs are much higher for aggregated Pt(II) complexes bearing type-I [O^N^C^N] ligands (**Pt-X-1** and **Pt-X-2**) than for those bearing type-II [O^N^C^N] ligands (**Pt-X-3**, **Pt-X-4** and **Pt-X-5**) due to the structural distortion and therefore the large k_{nr} of the latter during the decay from excited state T_{1a} to ground state S_0. A NIR emission with λ_{max} exceeding 700 nm and an EQE of 11.19% at a driving current density of 100 mA cm^{-2} has been realized for the non-doped OLED with neat **Pt-X-1** as the EML. Red emission with λ_{max} of 661 nm, CIE coordinates of (0.63, 0.37) and an EQE of 21.75% at 1000 cd m^{-2} have been achieved with the device based on **Pt-X-5** dopant in a co-host EML with a 26 wt% doping concentration.

Experimental Section

Materials: MoO_3, TCTA, TAPC, and B3PYMPM were purchased from Luminescence Technology Corp. All of these materials were used as received. **Pt-X-1** to **Pt-X-5** were synthesized as we previous described[15-16] and purified by gradient sublimation before use.

Device Fabrication and Characterization: OLEDs were fabricated in a Kurt J. Lesker SPECTROS vacuum deposition system with a base pressure of 10^{-8} mBar. In the vacuum chamber, organic materials were thermally deposited in sequence at a rate of ~0.1 nm s^{-1}. The doping process in the emitting layer was realized by co-deposition technology. Afterwards, LiF (1.2 nm) and Al (100 nm) were thermally deposited at rates of 0.03 and 0.2 nm s^{-1}, respectively. Film thicknesses were determined *in situ* by calibrated oscillating quartz-crystal sensors. For doped devices, CIE coordinates, *L-J-V* and EL spectra were measured simultaneously with a programmable Keithley model 2400 source-meter measurement unit and a Konika Minalta CS-2000 spectroradiometer. EQE and PE of doped devices as well as CIE coordinates, EQE, and EL spectra of non-doped devices were measured using a Keithley

2400 source-meter and an absolute external quantum efficiency measurement system (C9920-12, Hamamatsu Photonics). All devices were characterized at room temperature without encapsulation except for those for device stability investigation. UV-curable sealant, cover glass and desiccant were used to encapsulate the OLEDs for stability investigation.

Supporting Information
Supporting Information is available from the Wiley Online Library or from the author.

Acknowledgements

We gratefully acknowledge the support from the Basic Research Program of Shenzhen (JCYJ20160229123546997, JCYJ20160530184056496, and JCYJ20170818141858021), the Innovation and Technology Fund (ITS/224/17FP), Hong Kong Research Grants Council, General Research Fund (17330416), the Theme-Based Research Scheme (T23-713/11) and the National Key Basic Research Program of China (2013CB834802).

Received: ((will be filled in by the editorial staff))
Revised: ((will be filled in by the editorial staff))
Published online: ((will be filled in by the editorial staff))

References

[1] C.-L. Ho, H. Li, W.-Y. Wong, *J. Organomet. Chem.* **2014**, *751*, 261.

[2] a) M. Cocchi, D. Virgili, V. Fattori, J. A. G. Williams, J. Kalinowski, *Appl. Phys. Lett.* **2007**, *90*, 023506; b) Y. Sun, C. Borek, K. Hanson, P. I. Djurovich, M. E. Thompson, J. Brooks, J. J. Brown, S. R. Forrest, *Appl. Phys. Lett.* **2007**, *90*, 213503; c) M. Cocchi, J. Kalinowski, D. Virgili, J. A. G. Williams, *Appl. Phys. Lett.* **2008**, *92*, 113302; d) T.-C. Lee, J.-Y. Hung, Y. Chi, Y.-M. Cheng, G.-H. Lee, P.-T. Chou, C.-C. Chen, C.-H. Chang, C.-C. Wu, *Adv. Funct. Mater.* **2009**, *19*, 2639; e) K. R. Graham, Y. Yang, J. R. Sommer, A. H. Shelton, K. S. Schanze, J. Xue, J. R. Reynolds, *Chem. Mater.* **2011**, *23*, 5305; f) E. Rossi, L. Murphy, P. L. Brothwood, A. Colombo, C. Dragonetti, D. Roberto, R. Ugo, M. Cocchi, J. A. G. Williams, *J. Mater. Chem.* **2011**, *21*, 15501; g) X. Wu, Y. Liu, Y. Wang, L. Wang, H. Tan, M. Zhu, W. Zhu, Y. Cao, *Org. Electron.*

2012, *13*, 932; h) R. Tao, J. Qiao, G. Zhang, L. Duan, C. Chen, L. Wang, Y. Qiu, *J. Mater. Chem. C* **2013**, *1*, 6446; i) H. Xiang, J. Cheng, X. Ma, X. Zhou, J. J. Chruma, *Chem. Soc. Rev.* **2013**, *42*, 6128; j) X. Cao, J. Miao, M. Zhu, C. Zhong, C. Yang, H. Wu, J. Qin, Y. Cao, *Chem. Mater.* **2015**, *27*, 96; k) J.-L. Liao, Y. Chi, C.-C. Yeh, H.-C. Kao, C.-H. Chang, M. A. Fox, P. J. Low, G.-H. Lee, *J. Mater. Chem. C* **2015**, *3*, 4910; l) S. Kesarkar, W. Mróz, M. Penconi, M. Pasini, S. Destri, M. Cazzaniga, D. Ceresoli, P. R. Mussini, C. Baldoli, U. Giovanella, A. Bossi, *Angew. Chem.* **2016**, *128*, 2764; *Angew. Chem. Int. Ed.* **2016**, *55*, 2714.

[3] a) L. Yao, S. Zhang, R. Wang, W. Li, F. Shen, B. Yang, Y. Ma, *Angew. Chem.* **2014**, *126*, 2151; *Angew. Chem. Int. Ed.* **2014**, *53*, 2119; b) X. Han, Q. Bai, L. Yao, H. Liu, Y. Gao, J. Li, L. Liu, Y. Liu, X. Li, P. Lu, B. Yang, *Adv. Funct. Mater.* **2015**, *25*, 7521; c) J. Xue, C. Li, L. Xin, L. Duan, J. Qiao, *Chem. Sci.* **2016**, *7*, 2888; d) G. Qian, Z. Zhong, M. Luo, D. Yu, Z. Zhang, Z. Y. Wang, D. Ma, *Adv. Mater.* **2009**, *21*, 111; e) Y. Yang, R. T. Farley, T. T. Steckler, S.-H. Eom, J. R. Reynolds, K. S. Schanze, J. Xue, *J. Appl. Phys.* **2009**, *106*, 044509.

[4] a) S. Wang, X. Yan, Z. Cheng, H. Zhang, Y. Liu, Y. Wang, *Angew. Chem.* **2015**, *127*, 13260; *Angew. Chem. Int. Ed.* **2015**, *54*, 13068; b) Y. Yuan, Y. Hu, Y.-X. Zhang, J.-D. Lin, Y.-K. Wang, Z.-Q. Jiang, L.-S. Liao, S.-T. Lee, *Adv. Funct. Mater.* **2017**, *27*, 1700986; c) Y.-K. Wang, S.-F. Wu, S.-H. Li, Y. Yuan, F.-P. Wu, S. Kumar, Z.-Q. Jiang, M.-K. Fung, L.-S. Liao, *Adv. Opt. Mater.* **2017**, *5*, 1700566; d) R. Nagata, H. Nakanotani, C. Adachi, *Adv. Mater.* **2017**, *29*. 1604265; e) D.-H. Kim, A. D'Aléo, X.-K. Chen, A. D. S. Sandanayaka, D. Yao, L. Zhao, T. Komino, E. Zaborova, G. Canard, Y. Tsuchiya, E. Choi, J. W. Wu, F. Fages, J.-L. Brédas, J.-C. Ribierre, C. Adachi, *Nat. Photon.* **2018**, *12*, 98; f) Y. Hu, Y. Yuan, Y.-L. Shi, D. Li, Z.-Q. Jiang, L.-S. Liao, *Adv. Funct. Mater.* **2018**, *28*, 1802597.

[5] a) R. J. Curry, W. P. Gillin, *Appl. Phys. Lett.* **1999**, *75*, 1380; b) J. Kido, Y. Okamoto, *Chem. Rev.* **2002**, *102*, 2357; c) R. G. Sun, Y. Z. Wang, Q. B. Zheng, H. J. Zhang, A. J. Epstein, *J. Appl. Phys.* **2000**, *87*, 7589.

[6] a) T. T. Steckler, O. Fenwick, T. Lockwood, M. R. Andersson, F. Cacialli, *Macromol. Rapid Commun.* **2013**, *34*, 990; b) M. Sun, X. Jiang, W. Liu, T. Zhu, F. Huang, Y. Cao, *Synth. Met.* **2012**, *162*, 1406; c) B. C. Thompson, L. G. Madrigal, M. R. Pinto, T.-S. Kang, K. S. Schanze, J. R. Reynolds, *J. Polym. Sci. Part A: Polym. Chem.* **2005**, *43*, 1417; d) R. Yang, R. Tian, J. Yan, Y. Zhang, J. Yang, Q. Hou, W. Yang, C. Zhang, Y. Cao, *Macromol.* **2005**, *38*, 244.

[7] M. Cocchi, D. Virgili, V. Fattori, D. L. Rochester, J. A. G. Williams, *Adv. Funct. Mater.* **2007**, *17*, 285.

[8] a) S.-Y. Kim, W.-I. Jeong, C. Mayr, Y.-S. Park, K.-H. Kim, J.-H. Lee, C.-K. Moon, W. Brütting, J.-J. Kim, *Adv. Funct. Mater.* **2013**, *23*, 3896; b) K.-H. Kim, J.-Y. Ma, C.-K. Moon, J.-H. Lee, J. Y. Baek, Y.-H. Kim, J.-J. Kim, *Adv. Opt. Mater.* **2015**, *3*, 1191; c) K. H. Kim, J. L. Liao, S. W. Lee, B. Sim, C. K. Moon, G. H. Lee, H. J. Kim, Y. Chi, J. J. Kim, *Adv. Mater.* **2016**, *28*, 2526; d) T.-H. Han, Y. Lee, M.-R. Choi, S.-H. Woo, S.-H. Bae, B. H. Hong, J.-H. Ahn, T.-W. Lee, *Nat. Photon.* **2012**, *6*, 105; e) K. Udagawa, H. Sasabe, F. Igarashi, J. Kido, *Adv. Opt. Mater.* **2016**, *4*, 86; f) K.-H. Kim, S. Lee, C.-K. Moon, S.-Y. Kim, Y.-S. Park, J.-H. Lee, J. Woo Lee, J. Huh, Y. You, J.-J. Kim, *Nat. Commun.* **2014**, *5*; g) C. W. Lee, J. Y. Lee, *Adv. Mater.* **2013**, *25*, 5450.

[9] S. D. Cummings, R. Eisenberg, *J. Am. Chem. Soc.* **1996**, *118*, 1949.

[10] Q. Wang, I. W. Oswald, X. Yang, G. Zhou, H. Jia, Q. Qiao, Y. Chen, J. Hoshikawa-Halbert, B. E. Gnade, *Adv. Mater.* **2014**, *26*, 8107.

[11] J. R. Sommer, R. T. Farley, K. R. Graham, Y. Yang, J. R. Reynolds, J. Xue, K. S. Schanze, *ACS Appl. Mater. Interfaces* **2009**, *1*, 274.

[12] a) K. Tuong Ly, R.-W. Chen-Cheng, H.-W. Lin, Y.-J. Shiau, S.-H. Liu, P.-T. Chou, C.-S. Tsao, Y.-C. Huang, Y. Chi, *Nat. Photon.* **2017**, *11*, 63; b) Y. Nagai, H. Sasabe, J. Takahashi, N. Onuma, T. Ito, S. Ohisa, J. Kido, *J. Mater. Chem. C* **2017**, *5*, 527.

[13] a) M. Cocchi, J. Kalinowski, L. Murphy, J. A. G. Williams, V. Fattori, *Org. Electron.* **2010**, *11*, 388; b) X. Yang, F.-I. Wu, H. Haverinen, J. Li, C.-H. Cheng, G. E. Jabbour, *Appl. Phys. Lett.* **2011**, *98*, 033302; c) C.-W. Hsu, Y. Zhao, H.-H. Yeh, C.-W. Lu, C. Fan, Y. Hu, N. Robertson, G.-H. Lee, X. W. Sun, Y. Chi, *J. Mater. Chem. C* **2015**, *3*, 10837.

[14] M. P. a. C. E. Swenberg, *Electronic Processes in Organic Crystals and Polymers*, Oxford University Press, 1999.

[15] S. C. F. Kui, P. K. Chow, G. S. M. Tong, S.-L. Lai, G. Cheng, C.-C. Kwok, K.-H. Low, M. Y. Ko, C.-M. Che, *Chem. Eur. J.* **2013**, *19*, 69; b) G. Cheng, P.-K. Chow, S. C. F. Kui, C.-C. Kwok, C.-M. Che, *Adv. Mater.* **2013**, *25*, 6765.

[16] a) G. Cheng, S. C. F. Kui, W.-H. Ang, M.-Y. Ko, P.-K. Chow, C.-L. Kwong, C.-C. Kwok, C. Ma, X. Guan, K.-H. Low, S.-J. Su, C.-M. Che, *Chem. Sci.* **2014**, *5*, 4819; b) S. C. F. Kui, P. K. Chow, G. Cheng, C.-C. Kwok, C. L. Kwong, K.-H. Low, C.-M. Che, *Chem. Commun.* **2013**, *49*, 1497.

[17] a) Q. Hou, Y. Zhang, F. Li, J. Peng, Y. Cao, *Organometallics* **2005**, *24*, 4509; b) W. Zhuang, Y. Zhang, Q. Hou, L. Wang, Y. Cao, *J. Polym. Sci. Part A: Polym. Chem.* **2006**, *44*, 4174.

[18] Y.-S. Park, S. Lee, K.-H. Kim, S.-Y. Kim, J.-H. Lee, J.-J. Kim, *Adv. Funct. Mater.* **2013**, *23*, 4914.

[19] C. Adachi, M. A. Baldo, M. E. Thompson, S. R. Forrest, *J. Appl. Phys.***2001**, *9*, 5048.

[20] a) S. Reineke, K. Walzer, K. Leo, *Phys. Rev. B* **2007**, *75*, 125328; b) R. Coehoorn, H. van Eersel, P. Bobbert, R. Janssen, *Adv. Funct. Mater*. **2014**, 25, 2024.

High performance OLEDs are realized by using the aggregation form of [Pt(O^N^C^N)] complexes. EQEs of 11.19% at 100 mA cm^{-2} and 21.75% at 1000 cd m^{-2} were achieved in the NIR and red devices, respectively.

Keywords: platinum(II) complexes, deep-red emission, near-infrared emission, aggregation forms, organic light-emitting devices

Gang Cheng, Qingyun Wan, Wai-Hung Ang, Chun-Lam Kwong, Wai-Pong To, Pui-Keong Chow, Chi-Chung Kwok, and Chi-Ming Che*

High Performance Deep-Red/Near-Infrared OLEDs with Tetradentate [Pt(O^N^C^N)] Emitters in Aggregation Forms